ISIJ International, Vol. 45 (2005), No. 2, pp. 272–280

Impact Toughness and Tensile Properties Improvement through Microstructure Control in Hot Forged Nb–V Microalloyed Steel

Ali Reza KHODABANDEH, Mohammad JAHAZI,[1)] Steve YUE[2)] and Philippe BOCHER[3)]

Department of Materials Engineering, Tarbiat Modarres University, P.O.Box 14155-143 Tehran, Iran.
1) Aerospace Manufacturing Technology Center, Institute for Aerospace Research, National Research Council Canada, 5145 Decelles, H3T 2B2, Montreal, Quebec, Canada. 2) Department of Metals and Materials Engineering, McGill University, 3610 University St., H3A 2B2, Montreal, Quebec, Canada. 3) Département de Génie Mécanique, Ecole de Technologie Supérieure, 1100 Notre-Dame West, H3C 1K3, Montréal, Quebec, Canada.

(*Received on August 26, 2004; accepted in final form on November 16, 2004*)

The influence of thermomechanical processing parameters such as reheating temperature, deformation temperature, deformation percent and cooling rate on achieving high impact toughness properties was studied in a Nb–V microalloyed steel to be used as forged parts in automotive applications. 15 mm long and 65 mm diameter billets were forged using a 20 MN mechanical press. Tensile and Charpy impact tests specimens were machined out of the central part of the forged billets. The microstructure of the specimens was examined for each experimental condition using optical microscopy. Phase identification and distribution was studied using X-ray diffraction and orientation image microscopy techniques. The results indicate that, increasing the reheating temperature above the dissolution temperature of (Nb)(C, N) improved the impact energy values. By increasing the cooling rate from 0.3 to 3°C/s both tensile strength and impact toughness were improved. High elongation percent was also observed on samples reheated at higher temperature and/or cooled with the higher cooling rates. The obtained mechanical properties were related to the characteristics of microstructural components including acicular ferrite, retained austenite, pearlite and ferrite.

The interrelationship between thermomechanical processing parameters, microstructure development, and final mechanical properties were identified and optimized forging conditions to obtain high impact energy (>30 J) microalloyed forge steels were determined.

KEY WORDS: microalloy steel; mechanical properties; acicular ferrite; forging.

1. Introduction

Microalloyed forging steels were first introduced in late 70's.[1,2)] The incentive for the use of these steels has been the attainment of high yield and tensile strengths in the as forged condition, eliminating by this way the expensive and not environmentally friendly operation of quenching and tempering.[3,4)] However components made of microalloyed forging steels have always suffered from lower toughness values compared to their quenched and tempered counter parts. This has limited their applications particularly for safety components where both high strength and toughness properties are required.[2–6)] The first generation of microalloyed steels (C–Mn–V steels) had ferrite–pearlite microstructures and the low toughness values were associated to the inherent cleavage fracture mode of pearlite.[2,7–10)] Therefore researches have been focused on eliminating or minimizing the amount of pearlite that can be formed during post forge cooling.[2,7,11)] In recent years, the trend has been to modify the ferrite–pearlite microstructure with high impact toughness microstructures such as acicular ferrite through a judicious control of thermomechanical processing parameters. The ultimate objective of these attempts being the production of high strength-high toughness parts suitable for application in automobile safety parts.[7,12,13)]

Acicular ferrite is formed below the transformation temperature of proeutectoid ferrite and pearlite and above the martensite-start temperature. Therefore its transformation temperature range is similar to that of bainite. Although it has been reported that the transformation mechanism of bainite and acicular ferrite are similar; however their respective nucleation sites are different.[14–16)] In bainite, ferrite plates initiate at austenite grain boundaries, forming sheaves of parallel plates with the same crystallographic orientation.[17)] By contrast, it is well accepted that acicular ferrite is nucleated intragranularly on inclusions within large austenite grains and then radiates in many different directions.[17–19)] It has been also suggested that, acicular ferrite is in fact intragranularly nucleated bainite[18,19)] or it results from multiple impingement of various intragranular widmanstatten ferrite and intragranularly nucleated polygonal ferrite.[20)] The nucleation mode of acicular ferrite is such that it results to a chaotic arrangement of plates and fine grains interlocked, which leads to a microstructure that is less organized when compared with ordinary bainite.[21–23)] Such microstructures are better suited to deflect propagating cleavage cracks and therefore more desirable from toughness point of view.[17–19)]

© 2005 ISIJ

Table 1. Chemical composition of steel investigated (wt%).

C	Si	S	P	Mn	Cr	Ni	Cu	V	Nb	N
0.27	0.56	0.037	0.0168	1.4	0.16	0.12	0.19	0.09	0.055	0.007

The growth of ferrite plates results in carbon enrichment of the remaining austenite, which may remain untransformed or transform to martensite, bainite or interlath carbides. Upon the application of strain, the untransformed austenite is converted to martensite, which would increase strain hardening and residual compressive stresses bringing higher resistance to necking and crack arrest properties, respectively.[24] In the acicular ferrite microstructure, refining the ferrite lath size, eliminating pearlite, minimizing the development of interlath carbides, and control of the amount and distribution of retained austenite are critical for the achievement of optimum strength and toughness properties.[7,9,25]

In the present article the influence of thermomechanical process parameters on the above mentioned microstructural characteristics particularly with regard to the formation of acicular ferrite and the resultant mechanical properties of a Nb–V microalloyed steel is investigated. The overall objective of the study was the development of a forging process to produce high strength-high toughness (tensile strength $>$850 Mpa, impact energy at room temperature $>$30 J) microalloyed forged automotive safety parts such as axles, hubs and steering parts.

2. Material and Experimental Procedures

The material used in this investigation was a Nb–V microalloyed steel produced in an electric arc furnace equipped with semi-automatic charging system and oxy-gas burners. Secondary steelmaking operations were performed in a ladle furnace with vacuum degassing units to eliminate oxygen and nitrogen as well as inclusion modification capabilities. Continuous cast blooms were produced and then hot rolled to 65 mm diameter bars out of which the specimens used in this investigation were machined out. Steel bars were inspected by magnetic particles inspection method to identify and remove any possible surface cracks.

The chemical composition of the steel is given in **Table 1**. As indicated, carbon content is about 0.27% to exploit its strengthening effect. Si was added to prevent the formation of cementite and therefore pearlite, which are detrimental to toughness. The presence of Cu enhances acicular ferrite formation and finally V and Nb were added as microalloying elements to use their precipitation strengthening effects.

To reveal prior austenite grain boundaries and to determine the effect of reheating temperature on austenite grain size, specimens with 8 mm diameter and 12 mm height with their axis parallel to the axis of the bar were prepared from the as received material. They were then heated in an electrical furnace with SiC heating elements between 900 to 1 250°C for 10 min followed by water quenching. The specimens were then tempered at 550°C for 4 h to improve grain boundary etching. After usual grinding and polishing operations (240 to 1 200 grit SiC paper followed by 1 μm diamond paste) they were etched in a supersaturated solution of warm picric acid and water with the addition of cupric chloride. Digital pictures were prepared by using optical microscopy and average austenite grain sizes were measured using the linear intercept method according to ASTM E112 standard.

An extensive number of relationships have been proposed for the dissolution temperature of Nb carbonitrides in microalloyed steels.[26–31] In the present study, the above temperature was estimated using the following relationships proposed by Johansen (1), Hudd (2) and Narita (3) whose steel compositions are the closest to the one used in this work.[26–28]

$$\log[\mathrm{Nb}][\mathrm{C}]=(-9\,290/T)+4.37 \quad \text{.....(1)}$$

$$\mathrm{Log}[\mathrm{Nb}][\mathrm{C}]=(-10\,960/T)+5.43 \quad \text{.....(2)}$$

$$\mathrm{Log}[\mathrm{Nb}][\mathrm{C}]=(-7\,900/T)+3.42 \quad \text{.....(3)}$$

The above relationships lead to dissolution temperatures of 1 225°C (Eq. (1)), 1 237°C (Eq. (2)), and 1 232°C (Eq. (3)).

The effect of forging parameters on microstructure and mechanical properties was studied on 150$\times\Phi$65 mm billets from the as received rolled bars. The specimens were reheated to 1 200°C or 1 250°C in a continuous induction furnace for 5 min. The selection of the reheating temperature was made with the objective to study the effect of smaller austenite grain size and larger carbonitrides (reheating at 1 200°C) versus large austenite grain sizes and very fine carbonitrides (upon cooling from 1 250°C) on final mechanical properties. Optical pyrometry was used to measure the temperature of the billets at the exit of the induction coil. The specimens were then immediately deformed (for tests at 1 200 and 1 250°C) or cooled at a rate of 1°C/s to the selected deformation temperature (1 200 or 1 150°C) as shown schematically in **Fig. 1**(a). A 20 MN mechanical forging press was employed to apply percent height reductions (*i.e.* percent deformation) of 20, 50 and 75%. In order to simulate, as accurately as possible, the actual part forging operations, the billets were forged normal to their rolling directions (Fig. 1(b)). This configuration allowed also the machining of tensile and impact test samples out of the forged billets. The as forged billets were then cooled to room temperature with different cooling rates. These were bin cooled (0.3°C/s), air cooled (1°C/s), and forced air cooled (3°C/s). Temperature drop during cooling was followed by inserting an appropriate thermocouple into a 3 mm diameter hole drilled at a fixed distance near the central part of the billets (Fig. 1(b)).

Tensile and impact test specimens were prepared from the center of the deformed billets according to ASTM E8 and E23 standards, respectively. An instrumented tensile testing system (Shenk) and an automatic impact testing machine (Wolpert) were used for evaluating mechanical properties.

Metallography samples, perpendicular to the forging direction, were extracted from the extremities of the impact

© 2005 ISIJ

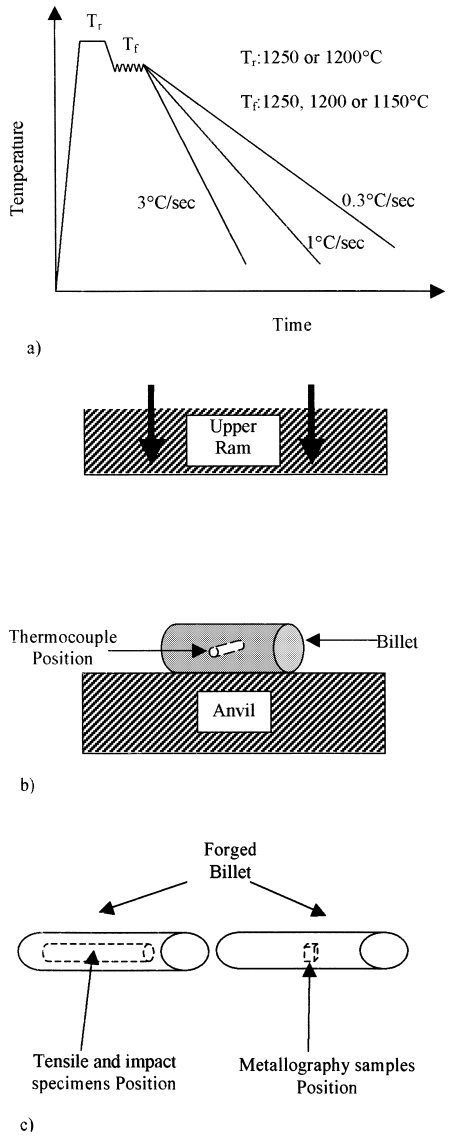

Fig. 1. (a) Schematical diagram of thermomechanical processing, (b) specimen and thermocouple's position during forging, and (c) location of mechanical and metallugraphical samples in forged billet.

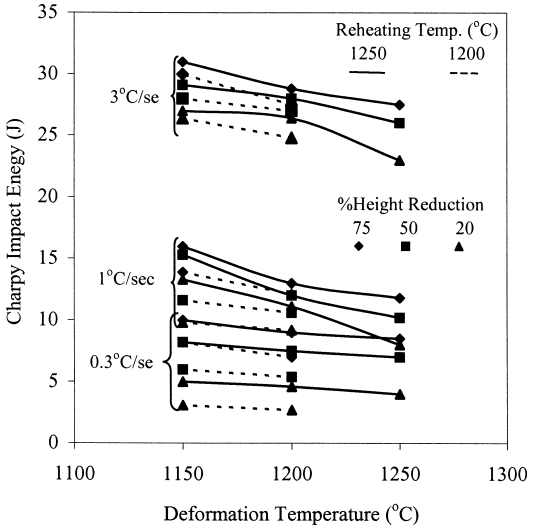

Fig. 2. Variation of Charpy impact energy with forging parameters.

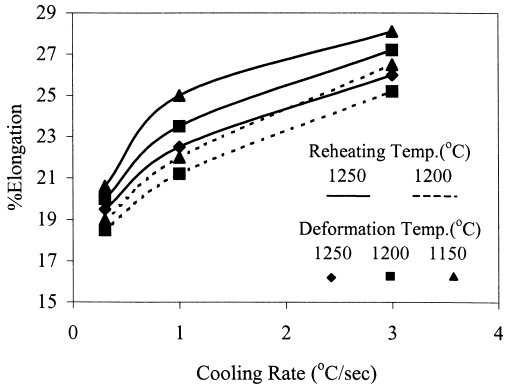

Fig. 3. Variation of % elongation with cooling rate, reheating and deformation temperatures.

test specimens. They were then cold mounted in bakelite, polished, and etched with 5% nital. An optical microscope instrumented by image analysis software was used for microstructure examination. The volume percent of phases was measured by point counting method according to ASTM E562 and color etching using sodium metabisulphite revealed the retained austenite in microstructure. Finally, orientation image microscopy (OIM) and X-ray diffraction methods were used to confirm the presence of retained austenite and to calculate its percentage in the final microstructure.

3. Results

3.1. Mechanical Properties

Figures 2 and **3** show the variation of Charpy impact energy and elongation percent with cooling rate, reheating and deformation temperatures as well as percent height reduction. The results indicate that, impact energy increases with increasing cooling rate, reheating temperature and percent height reduction but decreases with increasing deformation temperature. As indicated in Fig. 2(a) impact energy increases from 10 to 31 J when cooling rate increases from 0.3 to 3°C/s for billets reheated at 1 250°C and deformed 75% at 1 150°C. It is interesting to note that, for the latter cooling condition (*i.e.* 3°C/s) the elongation percent during tensile testing approaches 28%, which represents very good ductility. A similar behavior to impact energy and percent elongation was observed for the evolution of reduction of area for 1 250°C reheating temperature with cooling rate; *i.e.* it increased significantly (from 35 to 50.3%) by increasing cooling rate and decreasing deformation temperature.

However the specimens reheated at 1 200°C show different behavior. For instance, as shown in **Fig. 4** while the reduction of area is very high (~50%) with 0.3°C cooling rate, it decreases to about 40% for 1°C/s and then approaches 47% when the cooling rate is increased to 3°C/s. Reduction of area also improves by increasing percent height reduction and decreasing deformation temperature (from 1 200 to 1 150°C) as indicated in Fig. 4.

Engineering stress–strain curves of specimens with 75% height reduction are reported in **Fig. 5**. As can be observed, increasing cooling rate and reheating temperature extend the stress–strain curves; however the influence of varying the cooling rate appears to be more significant. Specifically,

© 2005 ISIJ

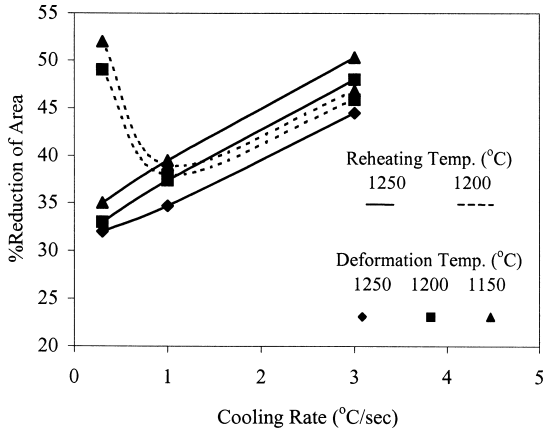

Fig. 4. Variation of % reduction of area with cooling rate.

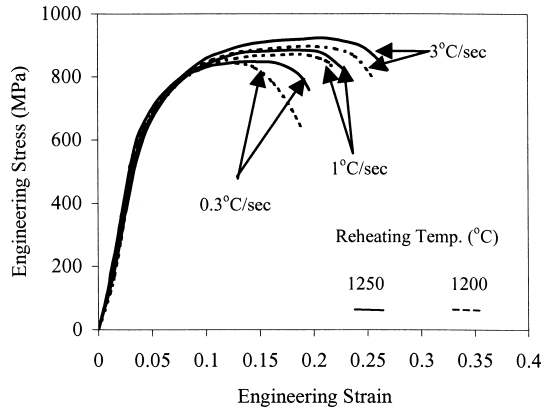

Fig. 5. Engineering stress–strain curves of specimens with 75% height reduction at 1 200°C.

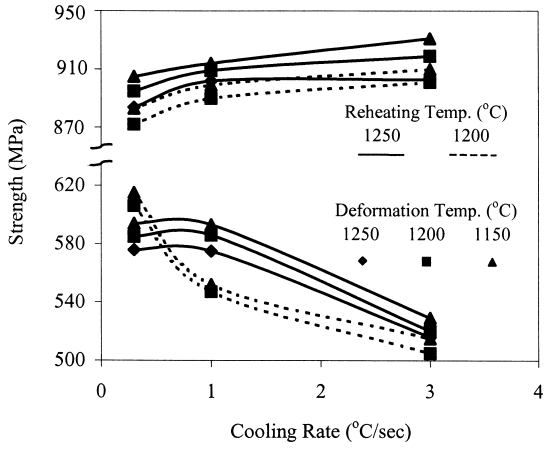

Fig. 6. Variation of yield and tensile strength with cooling rate.

specimens reheated at 1 200°C and cooled at 0.3°C/s represent larger post uniform strain zones (starting at strain of peak stress and finishing at fracture) and greater necking regions. By contrast those with the higher reheating temperature (1 250°C) and cooling rate (3°C/s) show larger uniform strains (the region between yield and peak stress) and lower post uniform strains.

The influence of thermomechanical processing parameters on yield and tensile strengths are illustrated in **Figs. 6** and **7**. The results indicate that, yield strength decreases with increasing cooling rate for both reheating temperatures while increasing cooling rate and reheating temperature results to higher tensile strength values. By contrast, as the

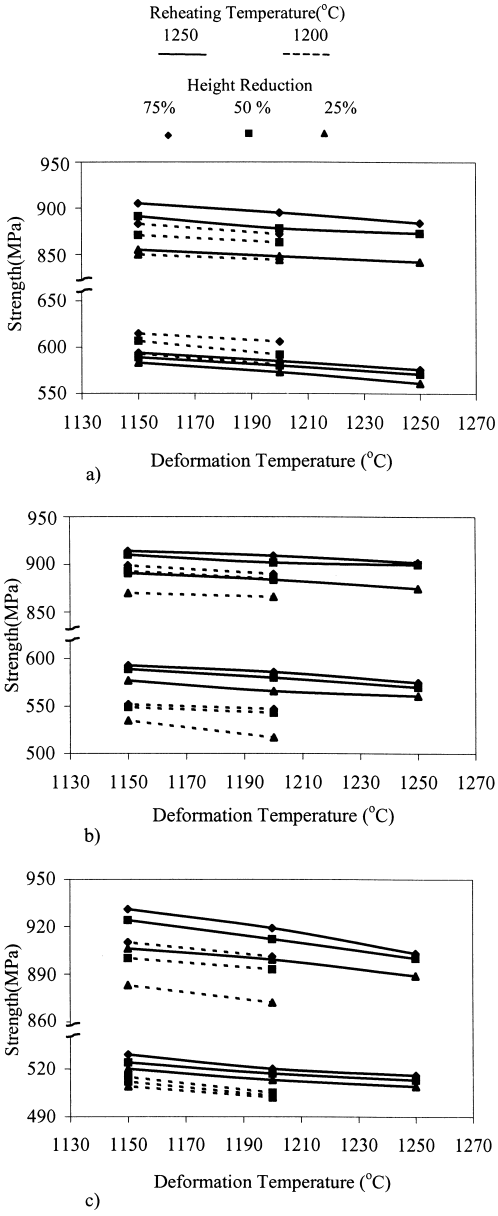

Fig. 7. Variation of yield and tensile strength with deformation temperature and percent height reduction at different cooling rates: (a) 0.3, (b) 1, and (c) 3°C/s.

deformation temperature is increased and/or the percent height reduction decreased both yield and tensile strengths are reduced to lower levels (Fig. 7).

3.2. Microstructure

Figure 8 shows the variation of mean austenite grain size with reheating temperature. As indicated, for reheating temperatures between 900 and 1 150°C the average austenite grain size increases slightly, passing from 9 μm at 900°C to 53 μm at 1 150°C. However, a sudden increase is observed at 1 200°C, which becomes even more important at 1 250°C where the average grain size reaches 171 μm. This clearly indicates that, the lower end dissolution temperature of (Nb)(C, N) precipitates is in the vicinity of 1 200°C and the upper end close to 1 250°C. The obtained results confirm that, the dissolution temperature of (Nb)(C, N) precipitates is in the interval 1200–1250°C as predicted based on relations reported previously.[26–28)]

© 2005 ISIJ

The influence of forging parameters on the propensity of the microstructure to produce acicular ferrite is illustrated in **Figs. 9**(a)–9(f). For instance, the microstructure of the samples reheated at 1 200°C, 75% height reduction and 0.3°C/s cooling rate is composed of ferrite and pearlite (Fig. 9(a)). By contrast, when the reheating temperature is increased to 1 250°C an acicular ferrite microstructure is obtained (Fig. 9(d)). The volume percent of the various phases was evaluated and the results are reported in **Fig. 10**. By increasing the reheating temperature to 1 250°C the volume percent of pearlite and granular ferrite decreases. The effect being more pronounced for pearlite (passing from 68 to 48%) than for granular ferrite (reduced from 32 to 21%). It is interesting to note that, under these conditions the volume percent of acicular ferrite increases from almost 0 to about 31%.

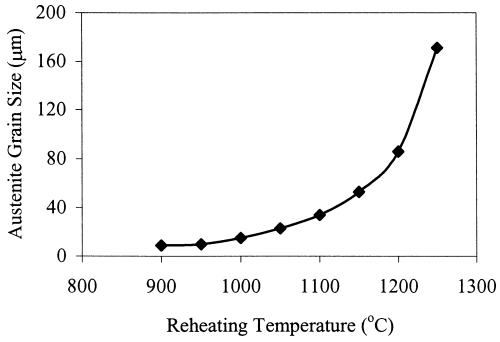

Fig. 8. Average austenite grain size variations with reheating temperature.

As the cooling rate is increased from 0.3 to 1°C/s, the volume percent of pearlite decreased from 68 to 24% and that of granular ferrite decreased from 32 to 19%, respectively (1 200°C reheating and deformation temperatures and 75% height reduction). At the same time, the content in acicular ferrite increased considerably passing from almost 0 to 57%. The effect of increasing reheating temperature or cooling rate on the final microstructure appears then to be similar. Also, as the cooling rate is increased to 1°C/s most of the interior of austenite grains is occupied by acicular

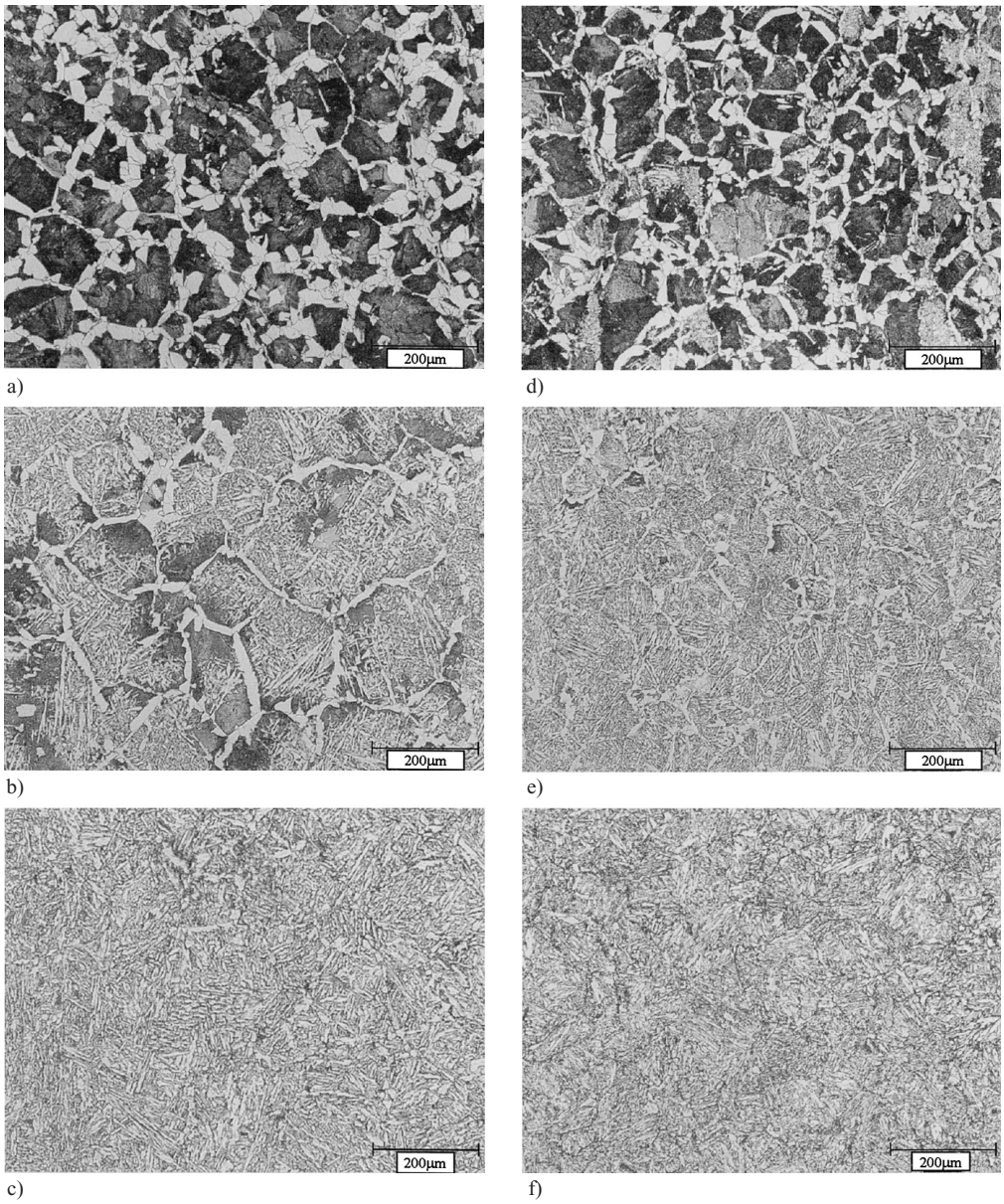

Fig. 9. Microstructures of specimens with 1 200°C (a)–(c) and 1 250°C (d)–(f) reheating temperatures, 75% height reduction at 1 200°C, and cooled at (a), (d) 0.3°C/s; (b), (e) 1°C/s; and (c), (f) 3°C/s.

© 2005 ISIJ

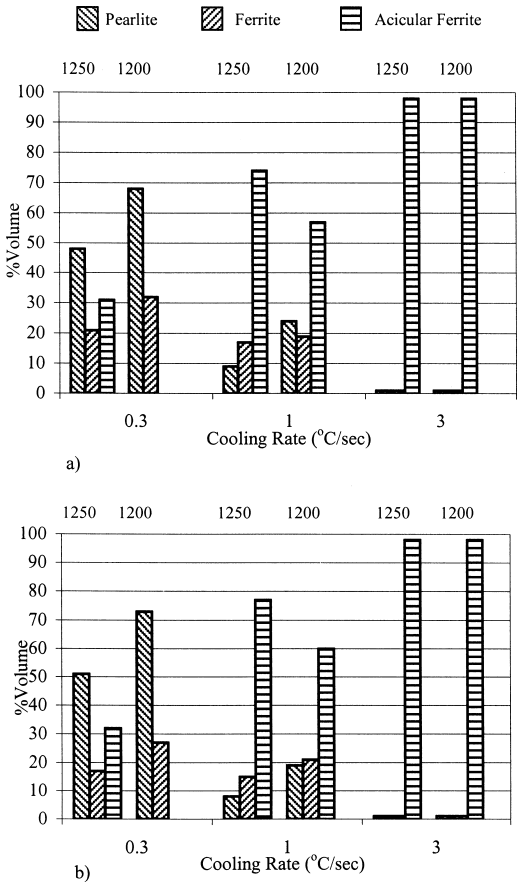

Fig. 10. Volume percent of phases for 75% deformation at (a) 1 200°C and (b) 1 150°C deformation temperatures (numbers on charts indicate reheating tmperatures (°C)).

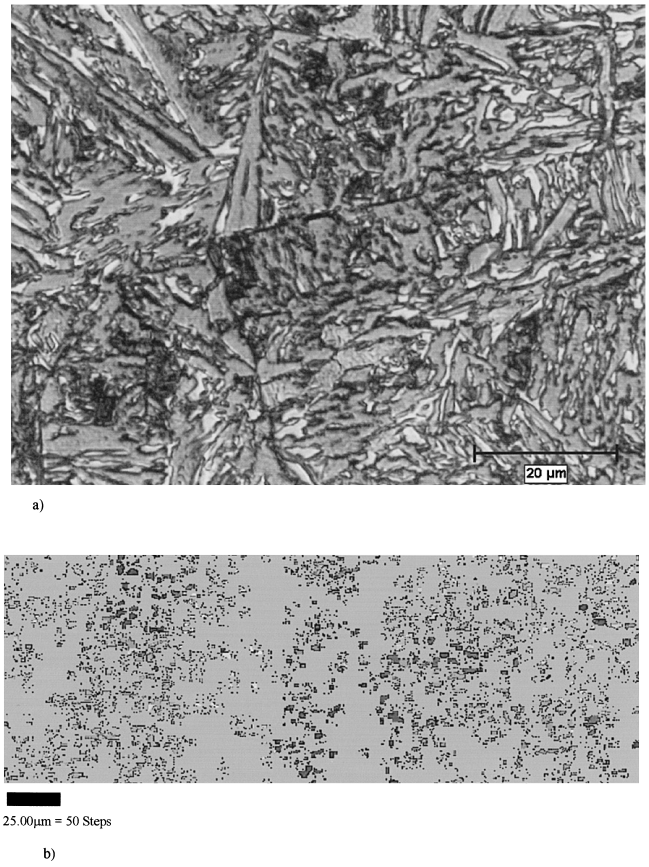

Fig. 11. Retained austenite, (a) revealed by color etching (white areas), (b) OIM (background is ferrite and all the islands and dark spots are austenite).

ferrite for both reheating temperatures (Figs. 9(b) and 9(e)). Increasing the cooling rate to 3°C/s eliminates almost all the pearlite and granular ferrite and replaces them by acicular ferrite as can be observed in Figs. 9(c) and 9(f). **Figures 11**(a) and 11(b) show an illustrative example of the presence and distribution of retained austenite revealed by color metallography (Fig. 11(a)) and OIM (Fig. 11(b)) in a billet solutionized at 1 250°C, deformed 75% at 1 200°C and cooled at 3°C/s. The volume percent of retained austenite was calculated by X-ray diffraction method. **Figure 12** shows the influence of reheating temperature and cooling rate on X-ray diffraction diagrams of the specimens. Using these diagrams, the volume percent of the retained austenite was calculated in each case and the results are reported in **Fig. 13**. As indicated, for 1 250°C reheating temperature and 75% deformation at 1 200°C, as the cooling rate is increased from 0.3 to 3°C/s the volume percent of retained austenite passes from 3 to 18%. By contrast, for the samples reheated and deformed at 1 200°C there is almost no retained austenite with the 0.3°C/s cooling rate, while the amount becomes near 17% at 3°C/s. This clearly indicates that, the effect of retained austenite is better revealed at lower cooling rates. The control of this constituent is of great importance to achieve high strength-high toughness properties.

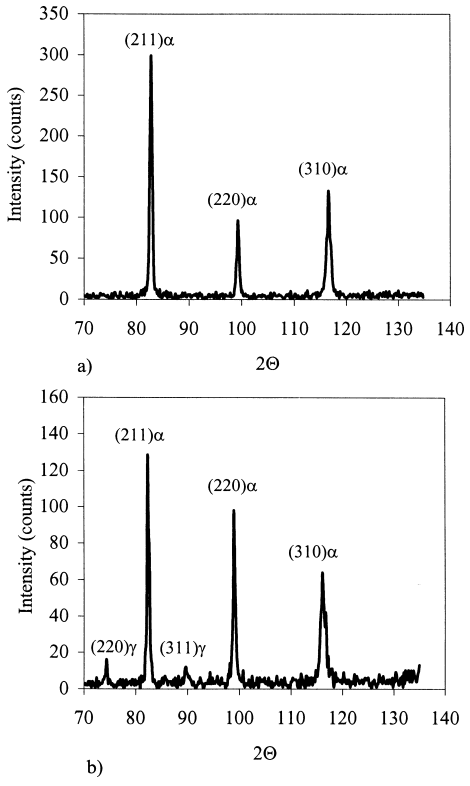

Fig. 12. X-ray diffraction diagrams of specimens deformed 75% at 1 200°C, reheating temperatures and cooling rates are (a) 1 200°C and 0.3°C/s, and (b) 1 250°C and 3°C/s.

© 2005 ISIJ

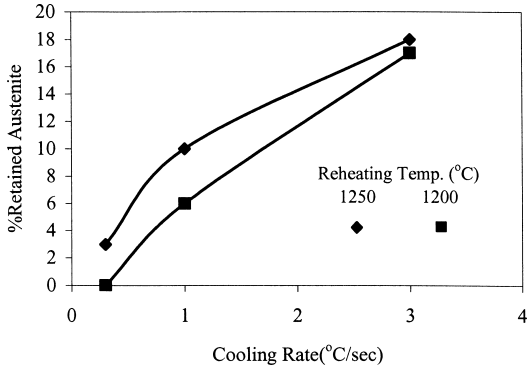

Fig. 13. Volume percent of retained austenite versus cooling rate.

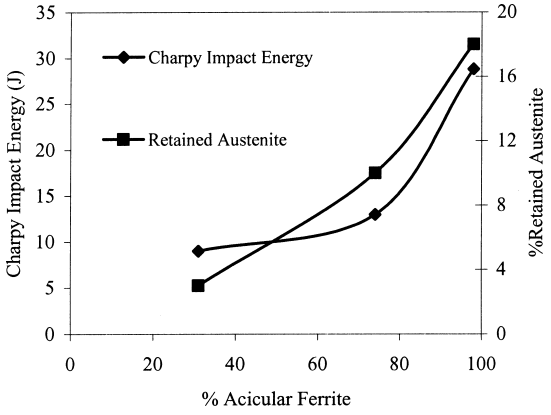

Fig. 14. Charpy impact energy and % retained austenite *versus* volume percent of acicular ferrite for specimens reheated at 1 250°C and deformed 75% at 1 200°C.

4. Discussion

4.1. Microstructure

4.1.1. Influence of Reheating Temperature

At the higher reheating temperature, the increase in the amount of acicular ferrite (Fig. 10) can be related to significantly higher austenite grain sizes of the specimen. Reheating at 1 200°C and 1 250°C, produces mean austenite grain sizes of 86 μm and 171 μm, respectively. With respect to transformation, austenite grain boundaries are preferred sites for the nucleation of proeutectoid ferrite, pearlite and bainite. Therefore, with larger austenite grains, fewer nucleation sites will be available for the above phases and the diffusion controlled transformation process becomes limited.[31,32] As a result, upon transformation, intragranular nucleation will be promoted in expense of grain boundary transformation products. It is well known that, acicular ferrite nucleates on inclusions located at the interior of austenite grains, by a combination of displacive and reconstructive mechanisms with less need to diffusion than products, such as ferrite and pearlite, that are diffusion controlled. Finally, because in hypoeutectoid steels, pearlite nucleates also at the interior of austenite grains, by initially increasing austenite grain size, the nucleation of acicular ferrite is promoted and the amount of pearlite is reduced as can be observed by comparing Figs. 9(a), 9(b) and 9(d), 9(e).

4.1.2. Influence of Percent Height Reduction and Deformation Temperature

Statically recrystallized austenite grain size, d^{γ} has been related to strain and deformation temperature by[33]:

$$d^{\gamma}=Bd_0^a\varepsilon^{-b}\exp[-Q/(RT)]$$

where, d_0 is the initial austenite grain size, ε is the total strain and T is the absolute temperature. Q and R are activation energy of recrystallization and gas constant, respectively. B, a and b are constants determined by the chemical composition of the steel. The above equation indicates that, decreasing deformation temperature and increasing strain decreases the statically recrystallized grain size. Finer recrystallized austenite grain size produces finer ferrite plates and packets upon transformation to acicular ferrite structures. Therefore, increasing percent height reduction and decreasing deformation temperature should produce finer acicular microstructures.[7] As illustrated in Fig. 10, under the same experimental conditions, an increase in the acicular ferrite content and a decrease in the volume percent of pearlite are observed.

4.1.3. Influence of Cooling Rate

Increasing cooling rate, decreases the diffusion time and reduces the transformation temperature, thus limiting the effectiveness of reconstructive mechanisms. Also, transformation at lower temperatures enhances displacive mechanisms and therefore promotes shear transformation products such as acicular ferrite, as shown in Figs. 9 and 10.

4.1.4. Retained Austenite

Pearlite is the most important carbon-consuming constituent in the microstructure. By decreasing the amount of this phase and replacing it by acicular ferrite, which has very low solubility for carbon, some austenite will remain in the final microstructure.[7,34] **Figure 14** shows that, increasing the volume percent of acicular ferrite and decreasing pearlite content, retained austenite content increased. Also ferrite plates surround retained austenite, giving them a platelike or granular morphology, as reported in Fig. 11. Finally the variation of percent retained austenite, calculated using X-ray diffraction as a function of testing conditions, was illustrated in Fig. 13. This variation alters the room temperature mechanical properties because of the differences in mechanical properties of austenite with ferrite and pearlite.

4.2. Mechanical Properties

4.2.1. Influence of Reheating Temperature and Cooling Rate

As reported in Fig. 2 for 75% reduction, Charpy impact energy increases with increasing cooling rate and reheating temperature. This can be attributed to the volume percent of pearlite and acicular ferrite as well as to the size of (Nb)(C, N) particles. Acicular ferrite has a chaotic type structure and its multidirectional thin plates deflect crack propagation whereas pearlite is susceptible to cleavage fracture. Thus, increasing acicular ferrite and decreasing pearlite, improves significantly impact toughness values. Specifically, increased acicular ferrite content obtained at higher cooling rates and reheating temperature should improve Charpy impact energy, as demonstrated in Fig. 14.

© 2005 ISIJ

On the other hand, at higher cooling rates where there is no obvious presence of pearlite (see Figs. 9(c), 9(f) and 10), the Charpy impact energy of specimens solutionized at 1 250°C is higher than those treated at 1 200°C. This behavior is probably related to larger Nb(C, N) particles that exist at 1 200°C, as this is below their dissolution temperature. It has been reported that, such particles can act as cleavage crack initiation points with a deleterious effect on impact energy.[9,35)]

As illustrated in Fig. 5, the engineering stress–strain curve, for specimen with 1 200°C reheating temperature and 0.3°C/s cooling rate, shows a sharp peak followed by a stress drop during necking accompanied with high post-uniform strain. Microstructural examination of the above specimens (Fig. 9(a)), showed a ferritic–pearlitic microstructure. The latter has a weak resistance to necking and the intense stress drop observed immediately after the peak is probably due to this feature. By contrast, specimens with 1 200°C reheating temperature and 3°C/s cooling rate did not show high post uniform strain, while presenting a high reduction of area. In these specimens and also in the specimens with 1 250°C reheating temperature and 3°C/s cooling rate, engineering stress–strain curves showed high uniform strain (*i.e.* higher percent elongation and reduction of area) and low post-uniform strain (Fig. 5).

The results reported in Fig. 4, show clearly that increasing the cooling rate up to 3°C/s increased reduction of area for both reheating temperatures to about 50%. The microstructures of these specimens (Figs. 9(c) and 9(f)) consisted of acicular ferrite with significant volume percent of retained austenite. The latter transforms to martensite during deformation, increasing plastic deformation and resulting to higher percent elongation and reduction of area. On the other hand, martensite has high resistance to necking and therefore specimens that contain higher amounts of retained austenite display extended engineering stress-strain curves and low post-uniform strain (*i.e.* smaller necking region), as indicated in Fig. 5.[36)]

The decrease in yield strength with increasing cooling rate, as observed in Fig. 6, can be related to the lower content of pearlite, the presence of low strength ferrite, and some austenite in agreement with results reported by other investigators.[7,24)] Also, the higher yield strength of specimens with 1 250°C reheating temperature compared to those reheated at 1 200°C can be related to the precipitation of NbC dissolved during reheating at 1 250°C, which does not exist at the lower reheating temperature. By contrast, the higher yield strength obtained for specimens reheated at 1 200°C and cooled with 0.3°C/s can be attributed to the presence of a higher volume percent of pearlite (Fig. 10). Therefore, at lower cooling rates where the microstructure consists mainly of pearlite, this constituent determines the yield strength; whereas, in microstructures consisting mainly of acicular ferrite, precipitates have the major role in determining the yield strength.

The increase in tensile strength with cooling rate observed for both reheating temperatures (Fig. 6), may be related to the transformation of retained austenite (presents in acicular ferrite) to martensite during uniform straining. The higher resistance of martensite to deformation increases strain hardening and ultimately the tensile strength.[7,24)]

5. Conclusions

(1) Thermomechanical processing parameters to obtain high strength-high impact toughness Nb–V forged microalloyed steels were optimized.

(2) Increasing reheating temperature from 1 200 to 1 250°C decreased considerably pearlite content, while the volume percent of acicular ferrite increased. The high volume fraction of acicular ferrite and retained austenite as well as the presence of very fine Nb(C, N) precipitates increases the impact toughness and tensile strength simultaneously.

(3) Increasing cooling rate decreases pearlite content and increases acicular ferrite volume percent. Increasing cooling rate up to 3°C/s produces acicular ferrite in expense of pearlite and granular ferrite. These microstructural variations increase impact energy, tensile strength, elongation percent and reduction of area of specimens with 1 250°C reheating temperature.

(4) Increasing percent height reduction and decreasing deformation temperature refines the microstructure and increases acicular ferrite content. These microstructural variations increase impact energy and the tensile properties.

Acknowledgements

The materials and testing facilities used in this investigation were kindly provided by Iran Tractor Forging Company. The authors would particularly thank Mr. R. Jadidi Managing Director of the company, Mr. S. T. Aghdashi and Mr. Nematkhah for their continual support throughout the projet. One of the authors, A. R. Khodabandeh, is grateful to McGill University for the provision of a visiting scientist fellowship.

REFERENCES

1) S. Gunnarson, H. Ravenshorst and C. M. Bergstrom: Proc. Fundamentals of Microalloying Forging Steels Conf., AIME, USA, (1987), 325.
2) W. A. Szilva, K. J. Grassl, J. W. Weith and P. H. Wright: Proc. Microalloyed Bar and Forging Steels Conf., TMS, Warrendale, PA, (1990), 227.
3) Y. Koyasu, H. Shinozaki, N. Ishii, N. Suzuki and A. Sakaguchi: *Nippon Steel Tech. Rep.*, **30** (1986), 20.
4) T. Shiragha, S. Suzuki, H. Kido, K. Matsumoto, M. Ishiguro and T. Abe: *NKK Tech. Rev.*, **53** (1988), 1.
5) Y. Koyasu, T. Takahashi, N. Ishii, H. Takada and H. Takeda: *Nippon Steel Tech. Rep.*, **47** (1990), 37.
6) S. T. Aghdashi, A. R. Khodabandeh and M. Jahazi: Proc. 4th Int. Conf. on HSLA Steels, HSLA '2000, The Metallurgical Industry Press, China, (2000), 404.
7) N. E. Aloi, G. Krauss, D. K. Matlock, C. I. Van Tyne and Y. W. Cheng: Proc. 36th MWSP Conf., TMS, Warrendale, PA, (1995), 201.
8) M. J. Balart, C. L. Davis and M. Strangewood: *Mater. Sci. Eng. A*, **A328** (2002), 48.
9) M. A. Linaza, J. L. Romero, J. M. Rodriguez-Ibabe and J. J. Urcola: *Scr. Metall. Mater.*, **29** (1993), 1217.
10) A. J. Nagy, G. Krauss, D. K. Matlock and S. W. Thompson: Proc. 36th MWSP Conf., TMS, Warrendale, PA, (1995), 271.
11) H. K. D. H. Bhadeshia: *Mater. Sci. Forum*, **284** (1998), 39.
12) D. K. Matlock, G. Krauss and J. G. Speer: *J. Mater. Process. Technol.*, **117** (2001), 324.
13) I. Madariaga, I. Gutierrez, C. Garcia-de Andres and C. Capdevila: *Scr. Mater.*, **41** (1999), 229.
14) B. L. Bramfitt and J. G. Speer: *Metall. Trans.*, **21A** (1991), 817.
15) M. Diaz-Fuentes and I. Gutierrez: *Mater. Sci. Eng. A*, **A363** (2003), 316.

© 2005 ISIJ

16) I. Madariaga, I. Gutierrez and H. K. D. H. Bhadeshia: *Metall. Mater. Trans. A*, **32A** (2001), 2187.
17) C. H. Lee, H. K. D. H. Bhadeshia and H. C. Lee: *Mater. Sci. Eng. A*, **A360** (2003), 249.
18) J. M. Gregg and H. K. D. H. Bhadeshia: *Acta Mater.*, **45** (1997), 739.
19) M. Diaz-Fuentes, A. Iza-Medina and I. Gutierrez: *Metall. Mater. Trans. A*, **34A** (2003), 2505.
20) G. Thewlis: *Mater. Sci. Technol.*, **20** (2004), 143.
21) I. Madariaga and I. Gutierrez: *Acta Mater.*, **47** (1999), 951.
22) J. S. Byun *et al.*: *Mater. Sci. Eng. A*, **A319** (2001), 326.
23) I. Madariaga, J. L. Romero and I. Gutierrez: *Metall. Mater. Trans.*, **29A** (1998), 1003.
24) A. J. Bailey, G. Krauss, S. W. Thompson, W. A. Szilva: Proc. 37th MWSP Conf., TMS, Warrendale, PA, (1996), 455.
25) S. W. Thompson and G. Krauss: Proc. 30th MWSP Conf., TMS, Warrendale, PA, (1989), 467.
26) T. J. Johansen, N. Christiensen and B. Augland: *Trans. Metall. Soc. AIME*, **239** (1967), 1661.
27) R. C. Hudd, A. Jones and M. N. Kale: *J. Iron Steel Inst.*, **209** (1971), 121.
28) K. Narita and S. Koyama: *Kobe Steel Eng. Rep.*, **18** (1966), 179.
29) H. Adrian: *Mater. Sci. Technol.*, **8** (1992), 406.
30) K. J. Irvine, F. B. Pickering and T. Gladman: *J. Iron Steel Inst.*, **205** (1967), 161.
31) R. P. Smith: *Trans. Metall. Soc. AIME*, **236** (1966), 220.
32) G. Krauss: Steels: Heat Treatment and Processing Principles, ASM, Ohio, (1990), 89.
33) H. K. D. H. Bhadeshia: Bainite in Steels, 2nd ed., The Institute of Materials, London, (2001), 237.
34) T. Siwecki, S. Zajac and G. Engberg: Proc. 37th MWSP Conf., TMS, Warrendale, PA, (1996), 721.
35) M. A. Linaza, J. L. Romero, J. M. Rodriguez-Ibabe and J. J. Urcola: *Scr. Metall. Mater.*, **32** (1995), 395.
36) K. Sugimoto, T. Iida, J. Sakaguchi and T. Kashima: *ISIJ Int.*, **40** (2000), 902.

© 2005 ISIJ